HAL
open science

Magnetotransport properties of polycrystalline La0.75Ho0.05Sr0.2MnO3

A Elghoul, A Krichene, Nassira Boudjada, W Boujelben

To cite this version:

A Elghoul, A Krichene, Nassira Boudjada, W Boujelben. Magnetotransport properties of polycrystalline La0.75Ho0.05Sr0.2MnO3. Bulletin of Materials Science, 2021, 44 (4), pp.274. 10.1007/s12034-021-02565-5 . hal-04179661

HAL Id: hal-04179661

https://hal.science/hal-04179661v1

Submitted on 10 Aug 2023

HAL is a multi-disciplinary open access archive for the deposit and dissemination of scientific research documents, whether they are published or not. The documents may come from teaching and research institutions in France or abroad, or from public or private research centers.

L'archive ouverte pluridisciplinaire **HAL**, est destinée au dépôt et à la diffusion de documents scientifiques de niveau recherche, publiés ou non, émanant des établissements d'enseignement et de recherche français ou étrangers, des laboratoires publics ou privés.

Bull. Mater. Sci. (2021) 44:274
https://doi.org/10.1007/s12034-021-02565-5

© Indian Academy of Sciences

Magnetotransport properties of polycrystalline $La_{0.75}Ho_{0.05}Sr_{0.2}MnO_3$

A ELGHOUL[1], A KRICHENE[1,*], N CHNIBA BOUDJADA[1,2] and W BOUJELBEN[1]
[1]Laboratoire de Physique des Matériaux, Faculté des Sciences de Sfax, Université de Sfax, 3000 Sfax, Tunisia
[2]Institut Néel, 38042 Grenoble Cedex 9, France
*Author for correspondence (akramkri@hotmail.fr)

MS received 9 May 2021; accepted 3 August 2021

Abstract. In this study, we have tried to simulate both temperature and magnetic field dependence of electrical resistivity for polycrystalline $La_{0.75}Ho_{0.05}Sr_{0.2}MnO_3$. The studied sample was elaborated by sol–gel method. The energy-dispersive X-ray confirms the presence of Ho element. The temperature dependence of resistivity in the whole temperature range (100–300 K) was successfully fitted by phenomenological percolation model, testifying the percolative nature of the electrical transition. The evolution of the volume fraction of the ferromagnetic phase is in agreement with the magnetic properties. The magnetic field dependence of resistivity follows the recently established universal behaviour of resistivity, which may confirm the validity of this model.

Keywords. Manganite; electrical resistivity; magnetoresistance; percolation model.

1. Introduction

The $Ln_{1-x}A_xMnO_3$ manganites (Ln is a rare-earth ion and A is divalent alkaline earth ion) demonstrate a great variety of fascinating properties, such as magnetoresistance (MR) and magnetocaloric effect, generally observed near the paramagnetic–ferromagnetic transition [1–4]. Several parameters may affect such transitions, such as the Mn^{3+}/Mn^{4+} ratio, the average ionic radius of the A-site $<r_A>$, the ionic size mismatch between the various A-site ions σ^2, the substituent nature and the sintering temperature [4–11]. The ferromagnetic behaviour can be interpreted by the double-exchange interactions between Mn^{3+} and Mn^{4+} ions via oxygen ions O^{2-}. Colossal MR in manganites can be ascribed to the phase separation phenomenon [3,12,13] and the percolative nature of the paramagnetic–ferromagnetic transition [14]. In order to explain the occurrence of resistivity maximum (metal–insulator transition), percolation model was proposed, based on magnetic phase separation mechanism [15]. This model suggests that the magnetic specimens are composed of ferromagnetic and paramagnetic phases coexisting together and that electrical resistivity values at any temperature are determined by the modification of the volume fractions of both coexisting phases.

Holmium-based manganites are very interesting to study [7,11,16–19]. Previous studies have been carried out on the $La_{0.75}Ho_{0.05}Sr_{0.2}MnO_3$ sample [16,17]. The magnetic study has revealed that our sample shows a ferromagnetic–paramagnetic transition near room temperature. The theoretical study has indicated the presence of short-range ferromagnetic interactions in this sample, corresponding to 3D-Ising model [17]. When studying the $La_{0.75}Ln_{0.05}Sr_{0.2}MnO_3$ system (with Ln = La, Sm, Eu, Gd, Dy and Ho), the Ho-based compound has demonstrated peculiar features (a relatively high Curie temperature value (near room temperature) and a considerable magnetocaloric effect for an important mismatch effect), which were attributed to the intrinsic contribution of Ho ions [16]. In this study, we have tried to investigate the magnetotransport properties of $La_{0.75}Ho_{0.05}Sr_{0.2}MnO_3$ sample by using the phenomenological percolation model.

2. Experimental

$La_{0.75}Ho_{0.05}Sr_{0.2}MnO_3$ compound was elaborated by sol–gel method by high-purity La_2O_3, Ho_2O_3, $SrCO_3$ and MnO_3. The synthesis procedure was previously detailed elsewhere [16]. X-ray powder diffraction was used for structural investigations at room temperature (Cu-Kα radiation source, λ = 1.5406 Å) in the 2θ range of 20°–80°. Our sample has been analysed by energy-dispersive X-ray analysis by analysing near-surface elements to estimate the elemental proportion at different positions. The temperature dependence of magnetization under 500 Oe applied magnetic field was carried out by using a vibrating sample magnetometer in the temperature range 5–330 K.

Published online: 30 October 2021

Resistivity measurements were carried out in the temperature rang 100–300 K under magnetic field values up to 2T using the standard four-probe method.

3. Results and discussion

The refinement of X-ray powder diffraction measurement of our studied sample is shown in figure 1. It is clear from the analysis that our sample is single phase with no detectable impurities and crystallizes in the orthorhombic structure with *Pnma* space group (N° 62). The unit cell parameters are a = 5.4762(2) Å, b = 7.7659(4) Å and c = 5.5213(2) Å with a unit cell volume equal to 234.8078 Å^3 [16]. Figure 2 shows the energy-dispersive X-ray of our studied compound. Energy-dispersive X-ray study confirms the existence of all elements in our sample and the absence of other elements. The atomic ratio of Ho element is 0.81% ± 0.04%. This value is very close to the theoretical one (1%), indicating the presence of Ho element and testifying the quality of our sample. In order to study the magnetic behaviour of our specimen, we have represented in figure 3 the temperature dependence of magnetization under 500 Oe applied magnetic field using field cooled (FC) and zero field cooled (ZFC) protocols. It can be seen that our sample exhibits a magnetic transition from ferromagnetic to paramagnetic state with increasing temperature at T_C = 307 K, corresponding to the minimum of dM_{FC}/dT as observed in the inset of figure 3. The T_C value suggests possible technological application at room temperature, like magnetic refrigeration, magnetic field sensing, bolometers and spintronics. The difference between FC and ZFC curves at low temperature may suggest the presence of a glassy state at low temperature. Further investigations are required in order to confirm the presence of such state.

The temperature dependence of resistivity for $La_{0.75}Ho_{0.05}Sr_{0.2}MnO_3$ sample under 0T, 1T and 2T magnetic fields is shown in figure 4. The sample exhibits a metal–insulator transition under 0T field around the transition temperature T_ρ = 201 K. T_ρ increases with increase in the applied magnetic field, due to enhancement of ferromagnetic interactions (double exchange mechanism). The T_C value is much higher than T_ρ, which means that some ferromagnetic domains may have an insulating behaviour above T_ρ. In order to understand the electrical behaviour in the ferromagnetic metallic phase ($T < T_\rho$), the electrical resistivity was fitted by Zener polynomial law given by [10]:

$$\rho_{FM} = \rho_0 + \rho_2 T^2, \tag{1}$$

where ρ_0 is the residual resistivity (temperature independent processes [20,21]) and $\rho_2 T^2$ is limited to electron–electron scattering mechanism [22]. The fitting of experimental resistivity in the metallic phase by using relation (1) is shown in figure 4. Thus, the conduction mechanism below T_ρ is essentially based on the contribution of electron–electron interactions. The temperature dependence of resistivity data above T_ρ for the studied sample has been analysed using small polaron hopping (SPH) model, described by the following relation [23]:

$$\rho_{PM} = AT\exp\left(\frac{E_a}{k_B T}\right), \tag{2}$$

where A is a constant, E_a the hopping energy and k_B the Boltzmann constant. The dashed lines in figure 4 confirm the validity of the chosen model. In order to describe the evolution of resistivity in the studied temperature range (especially in the vicinity T_ρ), we have used the phenomenological percolation model, which is based on magnetic phase segregation phenomenon. This model is based on the fact that the magnetic material contains a mixture of paramagnetic and ferromagnetic domains. According to this, the resistivity data can be analysed by the following relation [14]:

$$\rho = \rho_{FM} f + \rho_{PM}(1 - f), \tag{3}$$

where f and (1–f) are the volume fractions of ferromagnetic and paramagnetic regions, respectively. The volume fraction of the ferromagnetic phase satisfies the Boltzmann distribution, which can be written as:

$$f = \frac{1}{1 + \exp\left(\frac{\Delta U}{k_B T}\right)}, \tag{4}$$

where ΔU is the energy difference per unit cell between ferromagnetic metallic and paramagnetic insulating states. Since ΔU is temperature dependent, it can be developed to the first order as following [14]:

$$\Delta U = -U_0\left(1 - \frac{T}{T_C^{mod}}\right), \tag{5}$$

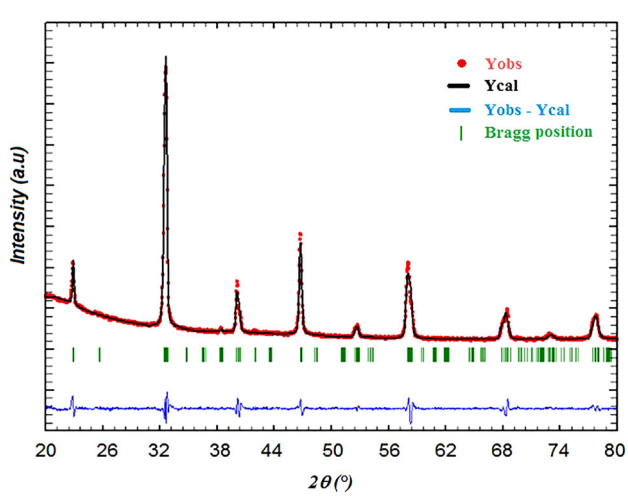

Figure 1. Reitveld fitted X-ray powder diffraction pattern of $La_{0.75}Ho_{0.05}Sr_{0.2}MnO_3$ sample.

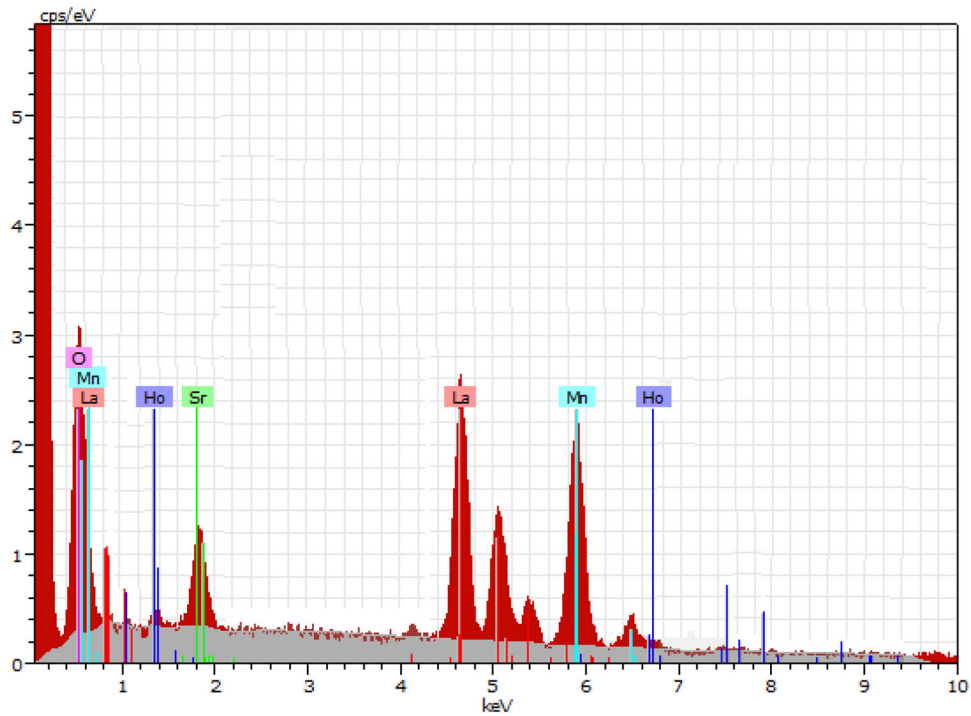

Figure 2. Energy-dispersive X-ray of $La_{0.75}Ho_{0.05}Sr_{0.2}MnO_3$ sample.

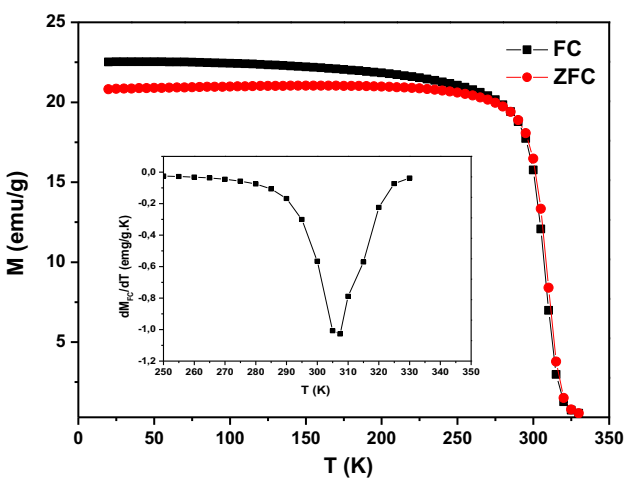

Figure 3. Temperature dependence of magnetization under an applied magnetic field of 0.05T of $La_{0.75}Ho_{0.05}Sr_{0.2}MnO_3$ sample. The inset shows the temperature dependence of dM_{FC}/dT.

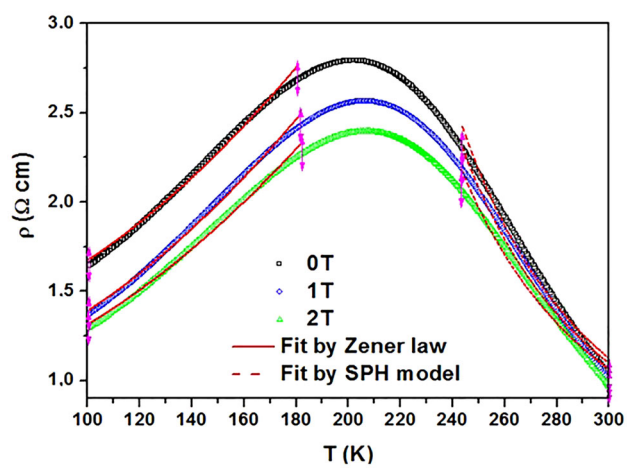

Figure 4. Temperature dependence of electrical resistivity for several values of applied magnetic field for $La_{0.75}Ho_{0.05}Sr_{0.2}MnO_3$ sample. Solid lines correspond to the fitting in the metallic phase and dashed lines correspond to the fitting in insulating phase.

According to this expression, T_C^{mod} is a characteristic temperature referring to the percolation threshold ($f = 1–f = 0.5$ at $T = T_C^{mod}$). By considering relations (1), (2) and (3), the percolation model for our sample can be described by:

$$\rho = f\left(\rho_0 + \rho_2 T^2 - AT\exp\left(\frac{E_a}{k_B T}\right)\right) + AT\exp\left(\frac{E_a}{k_B T}\right) \tag{6}$$

By replacing f by its expression using relations (4) and (5), relation (6) can be finally written as:

$$\rho = \frac{\left(\rho_0 + \rho_2 T^2 - AT\exp\left(\frac{E_a}{k_B T}\right)\right)}{1 + \exp\left[\frac{-U_0}{k_B}\left(\frac{1}{T} - \frac{1}{T_C^{mod}}\right)\right]} + AT\exp\left(\frac{E_a}{k_B T}\right) \tag{7}$$

Relation (7) was used to fit all the resistivity data in the whole temperature range 100–300 K for the different values of the applied magnetic field (0, 1 and 2T) and the fitted curves are shown in figure 5. It is worth mentioning that percolation model (relation (7)) is suitable to describe resistivity in the whole temperature range for our sample,

which is confirmed by the perfect match between theoretical and experimental curves (figure 5). The fitting parameters are summarized in table 1. From the fitting results, one can notice that changing the applied magnetic field value slightly affects the evolution of all the parameters. In fact, when the applied field increases, the residual resistivity ρ_0 and the electron–electron scattering coefficient ρ_2 decrease, indicating an amelioration of conductivity by the enhancement of the double exchange mechanism. Besides, we can observe a decrease of energy difference U_0 accompanied by an increase of T_C^{mod} with increase in the applied magnetic field. This fact is attributed to the enhancement of metallicity inside our compound. The decrease of E_a values indicates that electron hopping requires less energy due to the magnetic field, induced delocalization of charge carriers.

We have plotted on figure 6 the variation of the volume fraction of the ferromagnetic phase f, as a function of the temperature for our sample under 0, 1 and 2T fields. It is clear that $f(T)$ is equal to 1 below T_ρ, which confirms the strong dominance of the ferromagnetic metallic domains in this range. With increasing temperature up to T_C, f values are highly reduced due to the weakening of ferromagnetism. The important difference between T_C and T_ρ can be explained by percolation theory. In the temperature range $[T_\rho, T_C]$, f values decrease, which may generate some magnetic disorder that can explain the insulating behaviour. Previous studies have also shown the validity of percolation theory for other manganites [10,24–27].

Figure 7 shows the temperature dependence of MR under 1T and 2T fields for our sample. MR values has been calculated using the equation:

$$\mathrm{MR}(\%) = \frac{\rho(H) - \rho(0)}{\rho(0)} \times 100, \tag{8}$$

Table 1. Fitting results according to percolation model for $La_{0.75}Ho_{0.05}Sr_{0.2}MnO_3$ sample.

$\mu_0 H$ (T)	0	1	2
ρ_0 (Ω cm)	0.68	0.66	0.62
ρ_2 (10^{-5} Ω cm K^{-2})	0.5	0.3	0.1
A (10^{-6} Ω cm K^{-1})	2.53	2.61	2.80
E_a/k_B (K)	2166	2164	2151
U_0/k_B (K)	2266	2245	2230
T_C^{mod}(K)	257.8	259.6	261.6
T_ρ (K)	201	206	207

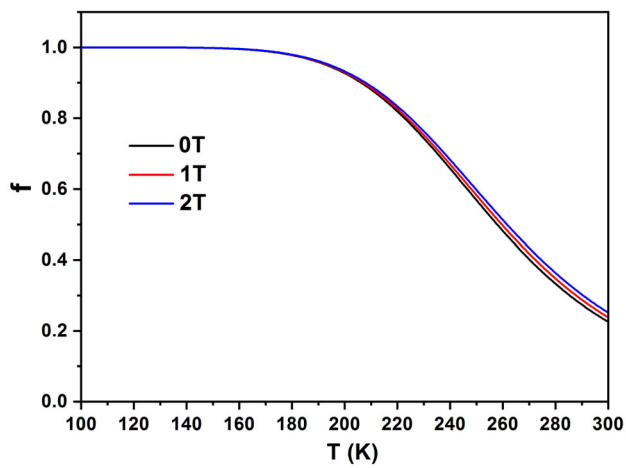

Figure 6. Temperature dependence of the volume fraction of the ferromagnetic phase for several values of applied magnetic field for $La_{0.75}Ho_{0.05}Sr_{0.2}MnO_3$ sample.

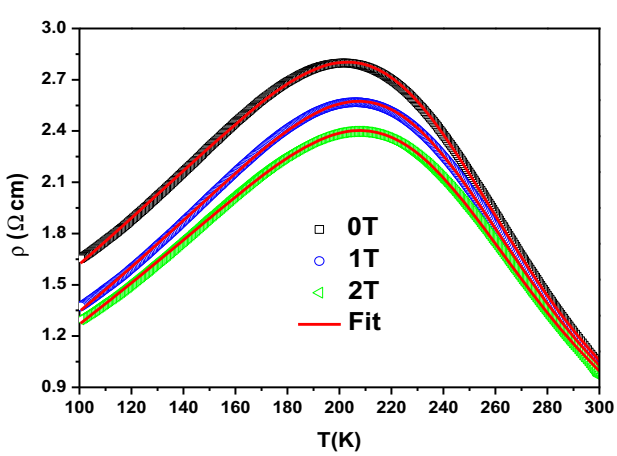

Figure 5. Temperature dependence of electrical resistivity for several values of applied magnetic field for $La_{0.75}Ho_{0.05}Sr_{0.2}MnO_3$ sample. The red curves represent the fitting using relation (7).

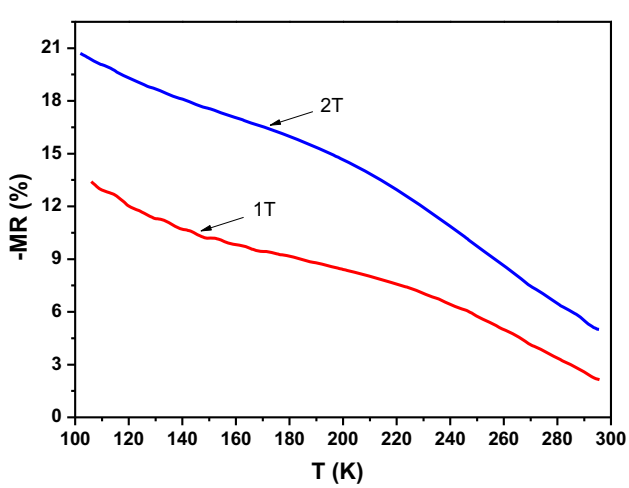

Figure 7. Temperature dependence of magnetoresistance under several values of applied magnetic field for $La_{0.75}Ho_{0.05}Sr_{0.2}MnO_3$ sample.

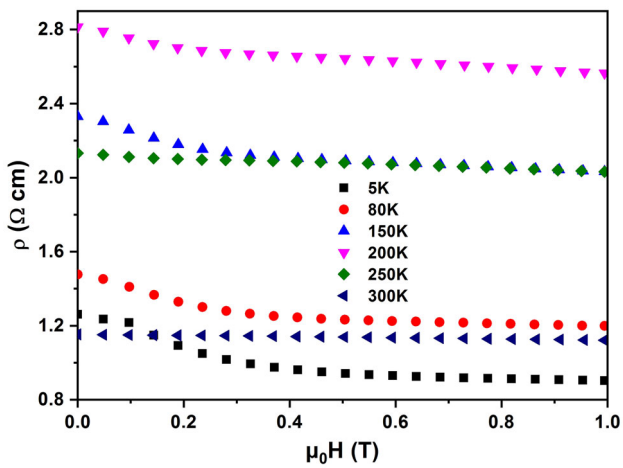

Figure 8. Magnetic field dependence of electrical resistivity recorded under several values of temperature for $La_{0.75}Ho_{0.05}Sr_{0.2}MnO_3$ sample.

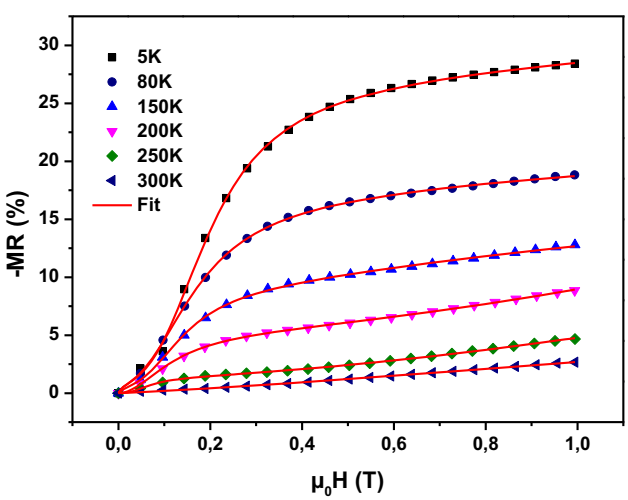

Figure 9. Magnetic field dependence of isothermal magnetoresistance for $La_{0.75}Ho_{0.05}Sr_{0.2}MnO_3$ sample. The red curves represent the fitting using relation (9).

where $\rho(H)$ and $\rho(0)$ are the resistivity, values under applied magnetic field H and in zero applied magnetic field, respectively. We can notice from figure 7, that our compound shows large MR values at a low temperature, which decrease with increase in temperature (under 2T field, – MR ∼ 21% at 100 K and – MR ∼ 5% at room temperature), indicating that MR effect can be ascribed to spin polarized tunneling phenomenon.

We have presented in figure 8 the evolution of resistivity *vs.* applied magnetic field at different temperature values for our specimen. The highest resistivity values were recorded at T_ρ. In addition, resistivity decreases with the increase in magnetic field from 0T to 1T for our sample, indicating a field-induced suppression in scattering mechanisms at grain boundaries. By using the data of figure 8 and relation (8), we have plotted in figure 9 the evolution of negative MR as a function of magnetic field for different temperature values. – MR(H) increases with applied field and decreases with increase in the temperature. We have recorded at 5 K around 29% of negative MR under 1T applied field.

Recently, a new model has been proposed to describe the magnetic field dependence of MR, which seems to be controlled by a universal law given by the following relation [28]:

$$-\mathrm{MR}(\mu_0 H) = \frac{K * H^p}{H_L^p + H^p} + \frac{(100 - K) * H^q}{H_H^q + H^q}, \quad (9)$$

where K is the amplitude of low-field MR (LFMR), $\mu_0 H_L$ and $\mu_0 H_H$ are critical field values linked to LFMR and high-field MR (HFMR), respectively, and p and q are critical exponents characterizing LFMR and HFMR, respectively. $\mu_0 H_L$ is the critical field required to achieve 50% of negative LFMR (LFMR = $K/2$ for $H = H_L$) and $\mu_0 H_L$ is the critical field required to achieve 50% of negative HFMR (HFMR = $(100 - K)/2$ for $H = H_H$). Figure 9 shows the fitted curves and the fitting results are summarized in table 2. From this table, we can notice that all the adjusted R^2-values ($\overline{R^2}$) are very close to 1, which confirm the fitting quality. We can also note that the LFMR amplitude K decreases with increase in the temperature and reaches zero at 300 K. According to the proposed model, K should be equal to 0 for $T \geq T_\rho$ [28]. However, $K \neq 0$ in the case of MR isotherms recorded at 200 and 250 K, which can be ascribed to the presence of ferromagnetism at these temperature values [10,28].

Table 2. Fitting parameters of the magnetic field dependence of MR using relation (8) for $La_{0.75}Ho_{0.05}Sr_{0.2}MnO_3$ sample.

T_ρ (K)	T (K)	K (%)	$\mu_0 H_L$ (T)	$\mu_0 H_H$ (T)	p	q	$\overline{R^2}$
201	5	22.08	0.010	10.75	2.87	0.57	0.999
	80	13.39	0.012	14.17	2.47	0.53	0.999
	150	6.18	0.003	13.37	2.91	0.68	0.999
	200	5.42	0.015	25.06	1.98	1.93	0.999
	250	1.31	0.002	27.45	2.44	1.66	0.999
	300	0.00	—	36.07	—	1.18	0.999

4. Conclusion

In this communication, we have investigated the magneto-transport properties in polycrystalline $La_{0.75}Ho_{0.05}Sr_{0.2}MnO_3$ prepared by sol–gel method. The magnetic study shows a paramagnetic–ferromagnetic transition near room temperature. The electrical resistivity in the entire temperature region (100–300K) has been fitted with the percolation theory. The perfect match between experimental and theoretical results confirms the percolative nature of the metal–insulator transition.

References

[1] Elghoul A, Krichene A, Chniba Boudjada N, Fettar F, Gay F and Boujelben W 2020 *J. Mater. Sci. Mater. Electron.* **31** 7076

[2] Elghoul A, Krichene A, Chniba Boudjada N and Boujelben W 2019 *Appl. Phys. A* **125** 780

[3] Krichene A, Boujelben W, Mukherjee S, Solanki P S and Shah N A 2017 *Acta Mater.* **131** 491

[4] Mabrouki W, Krichene A, Chniban Boudjada N and Boujelben W 2020 *Appl. Phys. A* **126** 182

[5] Elghoul A, Krichene A, Chniba Boudjada N and Boujelben W 2016 *J. Phys. Chem. Solids* **98** 263

[6] Qixiang S, Guiying W, Guoqing Y, Qiang M, Wenqi W and Zhensheng P 2008 *J. Rare Earth* **26** 821

[7] Rama N, Sankaranarayanan V and Rao M S R 2005 *J. Magn. Magn. Mater.* **292** 468

[8] Krichene A, Boujelben W and Cheikhrouhou A 2013 *J. Alloys Compd.* **550** 75

[9] Choudhary Y R S, Mangavati S, Patil S, Rao A, Nagaraja B S, Thomas R *et al* 2017 *J. Magn. Magn. Mater.* **451** 110

[10] Mabrouki W, Krichene A, Chniban Boudjada N and Boujelben W 2020 *J. Electron. Mater.* **49** 7024

[11] Bourouina M, Krichene A, Chniban Boudjada N and Boujelben W 2017 *Ceram. Int.* **43** 12311

[12] Dagotto E, Hotta T and Moreo A 2001 *Phys. Rep.* **344** 1

[13] Krichene A, Boujelben W, Mukherjee S, Shah N A and Solanki P S 2018 *J. Phys. Chem. Solids* **114** 21

[14] Li G, Zhou H D, Feng S L, Fan X J and Li X G 2002 *J. Appl. Phys.* **92** 1406

[15] Phong P T, Khiem N V, Dai N V, Manh D H, Hong L V and Phuc N X 2009 *J. Magn. Magn. Mater.* **321** 3330

[16] Elghoul A, Krichene A, Chniba Boudjada N and Boujelben W 2018 *Ceram. Int.* **44** 12723

[17] Elghoul A, Krichene A, Chniba Boudjada N and Boujelben W 2018 *Ceram. Int.* **44** 14510

[18] Raychaudhuri P, Nath T K, Sinha P, Mitra C, Nigam A K, Dhar S K *et al* 1997 *J. Phys.: Condens. Mater.* **9** 10919

[19] Dhieb S, Krichene A, Chniba Boudjada N and Boujelben W 2020 *J. Alloys Compd.* **823** 153728

[20] Urushibara A, Moritomo Y, Arima T, Asamitsu A, Kido G and Tokura Y 1995 *Phys. Rev. B* **51** 14103

[21] Worledge D C, Snyder G J, Beasley M R and Geballe T H 1996 *J. Appl. Phys.* **80** 5158

[22] Viret M, Ranno L and Coey J M D 1997 *Phys. Rev. B* **55** 8067

[23] Mott N F 1968 *J. Non-Cryst. Solids* **1** 1

[24] Krichene A, Bourouina M, Venkateshwarlu D, Solanki P S, Rayaprol S, Ganesan V *et al* 2016 *J. Magn. Magn. Mater.* **408** 116

[25] Christopher B, Rao A, Petwal V C, Verma V P, Dwivedi J, Lin W J *et al* 2016 *Physica B* **502** 119

[26] Venkatesh R, Yadam S, Venkateshwarlu D, Samatham S S, Bahl C R H and Pryds N 2015 *Mater. Chem. Phys.* **168** 74

[27] Xua L, Fana J, Zhu Y, Shi Y, Zhang L, Pi L *et al* 2015 *Chem. Phys. Lett.* **634** 174

[28] Krichene A, Boujelben W, Shah N A and Solanki P S 2020 *J. Alloys Compd.* **820** 153400